

On the Evolution of Universe using Relativistic Cosmology

Vigneswaran Ramamoorthy*

August 20, 2016

Abstract

For the collided region of two gravitationally bound structures A and B, geodesic equation is derived using calculus of variations. With the help of geodesic equation derived for the collided region of A and B, a method to calculate any possible curvature of universe beyond observable flat universe is detailed. This relativistic method is used to describe a generic idea on the evolution of gravitationally bound structures and its effect on the evolution of universe. Using this idea, distribution of matter and antimatter in the universe, observed accelerating expansion of universe, cosmic inflation, and large-scale structure of present universe are explained.

Key words: cosmology: theory — dark energy — early universe — inflation — large-scale structure of universe — methods: analytical

1 Introduction

In calculus of variations, the problem of finding shortest paths in a manifold and specifically, the problem of finding extremal of energy functional $E(\gamma)$ is used in this paper to derive geodesic equations. Considering two gravitationally bound structures A and B colliding with each other, geodesic equation for the collided region of A and B is derived using the problem of finding the critical points for energy functional. In section 4, A and B are assumed to collide in a flat region of universe. By using geodesic equation, derived for the collided region of A and B and three coordinate systems, x , y , and z , possible curvature beyond the flat region is calculated. This approach using geodesic equations is employed to derive an equation, which in specific explains the evolution of gravitationally bound structures and in general explains the evolution of universe. Though, this idea of evolution conceptually contradicts with the standard cosmological model, galaxy lattice (Susskind, 2013a) in standard model is supportively used here to explain the evolution of universe. Both cosmic inflation and accelerating expansion of universe follow naturally from this evolution pattern, and more importantly, from the gravitational forces itself. The widely known potential energy curve (Susskind, 2013b), which relates the hypothetical scalar field for cosmic inflation and dark energy for accelerating expansion, is juxtaposed with this evolution pattern for comparison. Distribution of matter and antimatter objects¹ is studied. Finally, large-scale structure of universe, as inferred from this evolution pattern and the meaning of curvature beyond observable flat universe in the context of this evolution, are discussed.

2 Finding Shortest Paths in a Manifold

To understand the problem of finding shortest paths in a manifold, here we employ the calculus of variations technique. Considering a simple problem where we are given a suitably differential function, $F : \mathbb{R} \times \mathbb{R} \times \mathbb{R} \rightarrow \mathbb{R}$, we seek among all functions $f(t) : [a, b] \rightarrow \mathbb{R}$, where $f(a) = a'$, $f(b) = b'$ one which will minimize or maximize the quantity $\int_a^b F(t, f(t), f'(t)) dt$.

To find maxima or minima for $J(f) = \int_a^b F(t, f(t), f'(t)) dt$, curves in the set of all functions $f(t) : [a, b] \rightarrow \mathbb{R}$ is considered. This is done by considering a variation of f , which is a function

*Address: No. 508/3, Mangal Nagar, Wakad Road, Shree Krishna Colony, Rajdep House, Thergaon, Pune, Maharashtra, India-411033. Orcid Id: 0000-0002-3356-3462 Email: vikipr@gmail.com Mobile: +91 9535471230

¹Objects refer to gravitationally bound structures.

$\alpha : (-\epsilon, \epsilon) \times [a, b] \rightarrow \mathbb{R}$, such that $\alpha(0, t) = f(t)$.

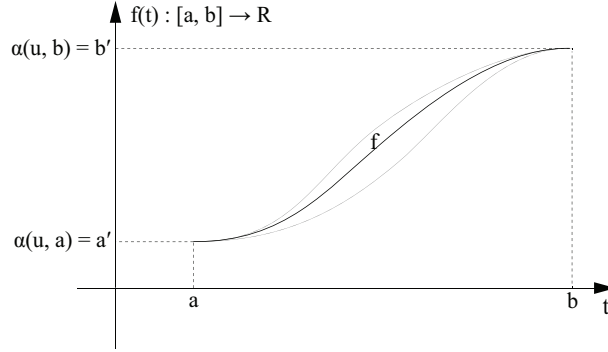


Figure 1: The Problem of finding shortest paths in a manifold is discussed here using calculus of variations method.

The functions $t \mapsto \alpha(u, t)$ here are a family of functions on $(-\epsilon, \epsilon)$ which pass through f for $u = 0$. This function is denoted by $\bar{\alpha}(u)$. So, $\bar{\alpha}(u)$ is a function from $(-\epsilon, \epsilon)$ to the set of functions $f(t) : [a, b] \rightarrow \mathbb{R}$. If $\alpha(u, a) = a'$ and $\alpha(u, b) = b'$ for all $u \in (-\epsilon, \epsilon)$, then we call α a variation of f keeping endpoints fixed. Computing $\left. \frac{dJ(\bar{\alpha}(u))}{du} \right|_{u=0}$, we get

$$\left. \frac{dJ(\bar{\alpha}(u))}{du} \right|_{u=0} = \int_a^b \frac{\partial \alpha(0, t)}{\partial u} \left[\frac{\partial F(t, f(t), f'(t))}{\partial x} - \frac{d}{dt} \left(\frac{\partial F(t, f(t), f'(t))}{\partial y} \right) \right] dt + \left. \frac{\partial \alpha(0, t)}{\partial u} \frac{\partial F(t, f(t), f'(t))}{\partial y} \right|_a^b$$

For variations α keeping end points fixed, second term is 0, and so

$$\left. \frac{dJ(\bar{\alpha}(u))}{du} \right|_{u=0} = \int_a^b \frac{\partial \alpha(0, t)}{\partial u} \left[\frac{\partial F(t, f(t), f'(t))}{\partial x} - \frac{d}{dt} \left(\frac{\partial F(t, f(t), f'(t))}{\partial y} \right) \right] dt$$

Generalizing the above considerations for functions $f(t) : [a, b] \rightarrow \mathbb{R}^n$ and $F : \mathbb{R} \times \mathbb{R}^n \times \mathbb{R}^n \rightarrow \mathbb{R}$, where the functional is $J(F) = \int_a^b F(t, f(t), f'(t)) dt$, variation of function $f(t)$ is a function $\alpha(u, t) : (-\epsilon, \epsilon) \times [a, b] \rightarrow \mathbb{R}^n$. $\alpha(u, t)$ is denoted by $\bar{\alpha}(u)$.

The general solution to find shortest paths in a manifold is that $f(t)$ should satisfy $\left. \frac{dJ(\bar{\alpha}(u))}{du} \right|_{u=0} = 0$, where

$$\left. \frac{dJ(\bar{\alpha}(u))}{du} \right|_{u=0} = \int_a^b \sum_{t=1}^n \frac{\partial \alpha^t(0, t)}{\partial u} \left[\frac{\partial F(t, f(t), f'(t))}{\partial x^t} - \frac{d}{dt} \left(\frac{\partial F(t, f(t), f'(t))}{\partial y^t} \right) \right] dt + \sum_{t=1}^n \left. \frac{\partial \alpha^t(0, t)}{\partial u} \frac{\partial F(t, f(t), f'(t))}{\partial y^t} \right|_a^b$$

For variations α keeping end points fixed, second term is 0, and so

$$\left. \frac{dJ(\bar{\alpha}(u))}{du} \right|_{u=0} = \int_a^b \sum_{t=1}^n \frac{\partial \alpha^t(0, t)}{\partial u} \left[\frac{\partial F(t, f(t), f'(t))}{\partial x^t} - \frac{d}{dt} \left(\frac{\partial F(t, f(t), f'(t))}{\partial y^t} \right) \right] dt \quad (1)$$

So, any critical point $f(t) : [a, b] \rightarrow \mathbb{R}^n$ of $J(F)$ (or an extremal for $J(F)$) must satisfy the n equations

$$\left[\frac{\partial F(t, f(t), f'(t))}{\partial x^t} - \frac{d}{dt} \left(\frac{\partial F(t, f(t), f'(t))}{\partial y^t} \right) \right] = 0$$

We can apply the above results to the problem of finding shortest paths in a manifold M .

$\gamma(t) : [a, b] \rightarrow M$ is a piecewise smooth curve, with $\gamma(a) = p$ and $\gamma(b) = q$, variation of γ here is a function $\alpha : (-\epsilon, \epsilon) \times [a, b] \rightarrow M$ for some $\epsilon > 0$, such that

(1) $\alpha(0, t) = \gamma(t)$,

(2) Partition $a = t_0 < t_1 < \dots < t_N = b$ of $[a, b]$ so that α is C^∞ on each strip $(-\epsilon, \epsilon) \times [t_{i-1}, t_i]$.

α is a variation of γ with endpoints fixed if

(3) $\alpha(u, a) = p$ and $\alpha(u, b) = q$ for all $u \in (-\epsilon, \epsilon)$

Now, we find the critical points for the energy functional, $E(\gamma(t)) = \frac{1}{2} \int_a^b \left\langle \frac{d\gamma}{dt}, \frac{d\gamma}{dt} \right\rangle dt$. $\bar{\alpha}(u)$ is the path $t \mapsto \alpha(u, t)$.

Analogous to the general solution above, here $\gamma(t)$ should satisfy $\left. \frac{dE(\bar{\alpha}(u))}{du} \right|_{u=0} = 0$, where

$$\left. \frac{dE(\bar{\alpha}(u))}{du} \right|_{u=0} = - \int_a^b \sum_{t=1}^n \frac{\partial \alpha^t(0, t)}{\partial u} \left[\sum_{r=1}^n g_{tr}(\gamma(t)) \frac{d^2 \gamma^r}{dt^2} + \sum_{i,j=1}^n [ij, t](\gamma(t)) \frac{d\gamma^i}{dt} \frac{d\gamma^j}{dt} \right] dt - \sum_{i=0}^N \left\langle \frac{\partial \alpha(0, t_i)}{\partial u}, \Delta_{t_i} \frac{d\gamma}{dt} \right\rangle$$

For variations α with end points fixed, the sum in the second term can be written from 1 to $N - 1$ and the integral term in the above equation is independent of the coordinate system.

$$\left. \frac{dE(\bar{\alpha}(u))}{du} \right|_{u=0} = - \int_a^b \sum_{t=1}^n \frac{\partial \alpha^t(0, t)}{\partial u} \left[\sum_{r=1}^n g_{tr}(\gamma(t)) \frac{d^2 \gamma^r}{dt^2} + \sum_{i,j=1}^n [ij, t](\gamma(t)) \frac{d\gamma^i}{dt} \frac{d\gamma^j}{dt} \right] dt \quad (2)$$

Where g_{tr} is the metric tensor and $[ij, t]$ is the Christoffel symbol of first kind containing first derivatives of the metric tensor.

$$[ij, t] = \frac{1}{2} \left(\frac{\partial g_{it}}{\partial x^j} + \frac{\partial g_{jt}}{\partial x^i} - \frac{\partial g_{ij}}{\partial x^t} \right)$$

So, any critical point $\gamma(t) : [a, b] \rightarrow M$ of $E(\gamma(t))$ (or an extremal for $E(\gamma(t))$) must satisfy the n equations

$$\left[\sum_{r=1}^n g_{tr}(\gamma(t)) \frac{d^2 \gamma^r}{dt^2} + \sum_{i,j=1}^n [ij, t](\gamma(t)) \frac{d\gamma^i}{dt} \frac{d\gamma^j}{dt} \right] = 0$$

A complete analysis on the problem of finding shortest paths in a manifold with the derivation of equations mentioned in this section is available in Spivak (1999). An interesting discussion on the motion of bodies in general relativity and how it differs from the motion of bodies in Newtonian methods is explained in Wisdom (2003). In the next section, equation (2) is used to derive an equation for the collided region of two gravitationally bound structures.

3 Equation of Motion in the Collided Region of Gravitationally Bound Structures

We will derive below the geodesic equation for the collided region of two gravitationally bound structures using the method of finding shortest paths in a manifold.

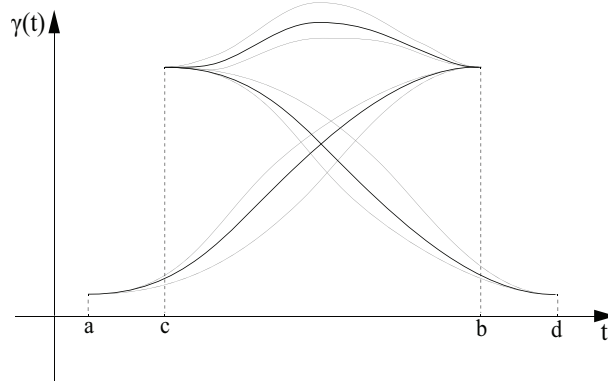


Figure 2: Collision of gravitationally bound structures; equation (2) is employed to derive an equation for the collided region, using the geodesic equations of two collided objects as shown here.

Adding the energy functional of these three paths, we get

$$E(\gamma(t))|_a^b + E(\gamma(t))|_c^b + E(\gamma(t))|_c^d = \frac{1}{2} \int_a^b \left\langle \frac{d\gamma}{dt}, \frac{d\gamma}{dt} \right\rangle dt + \frac{1}{2} \int_c^b \left\langle \frac{d\gamma}{dt}, \frac{d\gamma}{dt} \right\rangle dt + \frac{1}{2} \int_c^d \left\langle \frac{d\gamma}{dt}, \frac{d\gamma}{dt} \right\rangle dt$$

Here, equation (1) becomes

$$\begin{aligned} \frac{dJ(\bar{\alpha}(u))}{du} \Big|_{u=0} &= \int_a^b \sum_{t=1}^n \frac{\partial \alpha^t(0, t)}{\partial u} \left[\frac{\partial F(t, f(t), f'(t))}{\partial x^t} - \frac{d}{dt} \left(\frac{\partial F(t, f(t), f'(t))}{\partial y^t} \right) \right] dt \\ &+ \int_c^b \sum_{t=1}^n \frac{\partial \alpha^t(0, t)}{\partial u} \left[\frac{\partial F(t, f(t), f'(t))}{\partial x^t} - \frac{d}{dt} \left(\frac{\partial F(t, f(t), f'(t))}{\partial y^t} \right) \right] dt \\ &+ \int_c^d \sum_{t=1}^n \frac{\partial \alpha^t(0, t)}{\partial u} \left[\frac{\partial F(t, f(t), f'(t))}{\partial x^t} - \frac{d}{dt} \left(\frac{\partial F(t, f(t), f'(t))}{\partial y^t} \right) \right] dt \end{aligned}$$

Substituting equation (2) for the energy functional here, we get

$$\begin{aligned}
\left. \frac{dE(\bar{\alpha}(u))}{du} \right|_a^b + \left. \frac{dE(\bar{\alpha}(u))}{du} \right|_c^b + \left. \frac{dE(\bar{\alpha}(u))}{du} \right|_c^d = & - \int_a^b \sum_{t=1}^n \frac{\partial \alpha^t(0, t)}{\partial u} \left[\sum_{r=1}^n g_{tr}(\gamma(t)) \frac{d^2 \gamma^r}{dt^2} + \sum_{i,j=1}^n [ij, t](\gamma(t)) \frac{d\gamma^i}{dt} \frac{d\gamma^j}{dt} \right] dt \\
& - \int_c^b \sum_{t=1}^n \frac{\partial \alpha^t(0, t)}{\partial u} \left[\sum_{r=1}^n g_{tr}(\gamma(t)) \frac{d^2 \gamma^r}{dt^2} + \sum_{k,l=1}^n [kl, t](\gamma(t)) \frac{d\gamma^k}{dt} \frac{d\gamma^l}{dt} \right] dt \quad (3) \\
& 2 - \int_c^d \sum_{t=1}^n \frac{\partial \alpha^t(0, t)}{\partial u} \left[\sum_{r=1}^n g_{tr}(\gamma(t)) \frac{d^2 \gamma^r}{dt^2} + \sum_{m,n=1}^n [mn, t](\gamma(t)) \frac{d\gamma^m}{dt} \frac{d\gamma^n}{dt} \right] dt
\end{aligned}$$

For equation (3) to become 0, the condition below must hold.

$$\begin{aligned}
\left[\sum_{r=1}^n g_{tr}(\gamma(t)) \frac{d^2 \gamma^r}{dt^2} + \sum_{i,j=1}^n [ij, t](\gamma(t)) \frac{d\gamma^i}{dt} \frac{d\gamma^j}{dt} \right] + \left[\sum_{r=1}^n g_{tr}(\gamma(t)) \frac{d^2 \gamma^r}{dt^2} + \sum_{k,l=1}^n [kl, t](\gamma(t)) \frac{d\gamma^k}{dt} \frac{d\gamma^l}{dt} \right] \\
+ \left[\sum_{r=1}^n g_{tr}(\gamma(t)) \frac{d^2 \gamma^r}{dt^2} + \sum_{m,n=1}^n [mn, t](\gamma(t)) \frac{d\gamma^m}{dt} \frac{d\gamma^n}{dt} \right] = 0
\end{aligned}$$

Γ_{ij}^p , Γ_{kl}^p , and Γ_{mn}^p are introduced here to write the above equation in standard form.

$$\begin{aligned}
\Gamma_{ij}^p &= \sum_{t=1}^n g^{pt} [ij, t] = \sum_{t=1}^n g^{pt} \frac{1}{2} \left(\frac{\partial g_{ti}}{\partial x^j} + \frac{\partial g_{tj}}{\partial x^i} - \frac{\partial g_{ij}}{\partial x^t} \right) \\
\Gamma_{kl}^p &= \sum_{t=1}^n g^{pt} [kl, t] = \sum_{t=1}^n g^{pt} \frac{1}{2} \left(\frac{\partial g_{tk}}{\partial x^l} + \frac{\partial g_{tl}}{\partial x^k} - \frac{\partial g_{kl}}{\partial x^t} \right) \\
\Gamma_{mn}^p &= \sum_{t=1}^n g^{pt} [mn, t] = \sum_{t=1}^n g^{pt} \frac{1}{2} \left(\frac{\partial g_{tm}}{\partial x^n} + \frac{\partial g_{tn}}{\partial x^m} - \frac{\partial g_{mn}}{\partial x^t} \right)
\end{aligned}$$

Now, we get

$$\begin{aligned}
\left[\sum_{r=1}^n g^{pt} g_{tr}(\gamma(t)) \frac{d^2 \gamma^r}{dt^2} + \sum_{i,j=1}^n \Gamma_{ij}^p(\gamma(t)) \frac{d\gamma^i}{dt} \frac{d\gamma^j}{dt} \right] + \left[\sum_{r=1}^n g^{pt} g_{tr}(\gamma(t)) \frac{d^2 \gamma^r}{dt^2} + \sum_{k,l=1}^n \Gamma_{kl}^p(\gamma(t)) \frac{d\gamma^k}{dt} \frac{d\gamma^l}{dt} \right] \\
+ \left[\sum_{r=1}^n g^{pt} g_{tr}(\gamma(t)) \frac{d^2 \gamma^r}{dt^2} + \sum_{m,n=1}^n \Gamma_{mn}^p(\gamma(t)) \frac{d\gamma^m}{dt} \frac{d\gamma^n}{dt} \right] = 0
\end{aligned}$$

Simplifying the above equation, we get

$$\begin{aligned}
\left[\frac{d^2 \gamma^p}{dt^2} + \sum_{i,j=1}^n \Gamma_{ij}^p(\gamma(t)) \frac{d\gamma^i}{dt} \frac{d\gamma^j}{dt} \right] + \left[\frac{d^2 \gamma^p}{dt^2} + \sum_{k,l=1}^n \Gamma_{kl}^p(\gamma(t)) \frac{d\gamma^k}{dt} \frac{d\gamma^l}{dt} \right] \\
+ \left[\frac{d^2 \gamma^p}{dt^2} + \sum_{m,n=1}^n \Gamma_{mn}^p(\gamma(t)) \frac{d\gamma^m}{dt} \frac{d\gamma^n}{dt} \right] = 0
\end{aligned}$$

²In equation (3), n in subscript of \sum refers to n^{th} component of γ and n in superscript refers to summation limit. This holds for equations up to equation (4).

Rearranging the terms, we get equation of motion in the collided region of gravitationally bound structures A and B, which is

$$\left[\frac{d^2\gamma^p}{dt^2} + \sum_{k,l=1}^n \Gamma_{kl}^p(\gamma(t)) \frac{d\gamma^k}{dt} \frac{d\gamma^l}{dt} \right] = - \left[\frac{d^2\gamma^p}{dt^2} + \sum_{i,j=1}^n \Gamma_{ij}^p(\gamma(t)) \frac{d\gamma^i}{dt} \frac{d\gamma^j}{dt} \right] - \left[\frac{d^2\gamma^p}{dt^2} + \sum_{m,n=1}^n \Gamma_{mn}^p(\gamma(t)) \frac{d\gamma^m}{dt} \frac{d\gamma^n}{dt} \right] \quad (4)$$

Using this equation, an analytical method to calculate the curvature of universe beyond our observable is discussed below in section 4, and a generic evolution model is discussed in section 5.

4 Curvature Beyond Observable Flat Universe

We can consider the region in which the gravitationally bound structures collide to be flat, in a flat universe. So, the metric of Riemannian manifold is just a flat Euclidean metric on \mathbb{R}^n , which is

$$(\cdot, \cdot) = \sum_{i=1}^n g_{ij} dx^i \otimes dx^j$$

Equation of motion in the collided region is

$$\left[\frac{d^2\gamma^p}{dt^2} + \sum_{k,l=1}^n \Gamma_{kl}^p(\gamma(t)) \frac{d\gamma^k}{dt} \frac{d\gamma^l}{dt} \right] = - \left[\frac{d^2\gamma^p}{dt^2} + \sum_{i,j=1}^n \Gamma_{ij}^p(\gamma(t)) \frac{d\gamma^i}{dt} \frac{d\gamma^j}{dt} \right] - \left[\frac{d^2\gamma^p}{dt^2} + \sum_{m,n=1}^n \Gamma_{mn}^p(\gamma(t)) \frac{d\gamma^m}{dt} \frac{d\gamma^n}{dt} \right]$$

In flat Euclidean metric on \mathbb{R}^n , $g_{ij} = \delta_{ij}$. All the first derivatives of g_{ij} in the Christoffel symbols are 0, and so $\Gamma_{ij}^p = 0$, and $\Gamma_{mn}^p = 0$. Substituting $\Gamma_{ij}^p = 0$ and $\Gamma_{mn}^p = 0$ in the above equation, we get

$$\left[\frac{d^2\gamma^p}{dt^2} + \sum_{k,l=1}^n \Gamma_{kl}^p(\gamma(t)) \frac{d\gamma^k}{dt} \frac{d\gamma^l}{dt} \right] = - \left[\frac{d^2\gamma^p}{dt^2} + \frac{d^2\gamma^p}{dt^2} \right]$$

In flat Euclidean metric on \mathbb{R}^n , critical point $\gamma(t)$ for the energy function satisfy, $\frac{d^2\gamma^p}{dt^2} = 0$. Substituting $\frac{d^2\gamma^p}{dt^2} = 0$ in the above equation, we get

$$\left[\frac{d^2\gamma^p}{dt^2} + \sum_{k,l=1}^n \Gamma_{kl}^p(\gamma(t)) \frac{d\gamma^k}{dt} \frac{d\gamma^l}{dt} \right] = 0$$

4.1 Inference

1. Assumption is that universe is flat and so the region in which the gravitationally bound structures are about to collide is flat. After the collision, if curvature is observed in the collided region of gravitationally bound structures, then it is suggestive of a non-flat universe.

If after collision $\left[\frac{d^2\gamma^p}{dt^2} + \sum_{k,l=1}^n \Gamma_{kl}^p(\gamma(t)) \frac{d\gamma^k}{dt} \frac{d\gamma^l}{dt} \right] = 0$, the assumption that the universe is flat holds.

If after collision $\left[\frac{d^2\gamma^p}{dt^2} + \sum_{k,l=1}^n \Gamma_{kl}^p(\gamma(t)) \frac{d\gamma^k}{dt} \frac{d\gamma^l}{dt} \right] \neq 0$, the assumption that the universe is flat does not holds correct. In this case, the mathematical method to accurately calculate the curvature of universe is detailed in subsection 4.2.

4.2 Mathematical Method

Let the geometry of universe be defined by coordinate system x and the geometry of region in which the collision occurs be y . Coordinate system z defines the geometry of the collided region of gravitationally bound structures. Either of the images in fig. 3 illustrates the arrangement of coordinate systems.

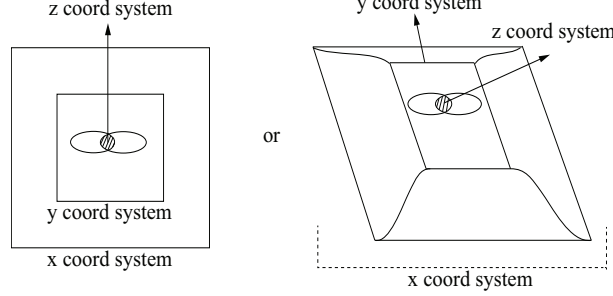


Figure 3: Relation between coordinate systems x , y , and z

First, we calculate the curvature of z coordinate system by comparing it with flat y coordinate system. Then, we calculate the curvature of x coordinate system by comparing it with the calculated curvature of z coordinate system.

Curvature of z coordinate system with respect to flat y coordinate system:

Metric equations which are needed to calculate Christoffel symbol Γ_{sn}^t are

$$g_{ls} = \sum_{\alpha} \frac{\partial z^{\alpha}}{\partial y^l} \frac{\partial z^{\alpha}}{\partial y^s}, \quad g_{ln} = \sum_{\alpha} \frac{\partial z^{\alpha}}{\partial y^l} \frac{\partial z^{\alpha}}{\partial y^n}, \quad g_{sn} = \sum_{\alpha} \frac{\partial z^{\alpha}}{\partial y^s} \frac{\partial z^{\alpha}}{\partial y^n}, \quad \text{and} \quad g^{tl} = \sum_{\beta} \frac{\partial y^t}{\partial z^{\beta}} \frac{\partial y^l}{\partial z^{\beta}} \quad (5)$$

First derivative of the metric equations with respect to y coordinate system components are as follows.

$$\frac{\partial g_{ls}}{\partial y^n} = \sum_{\alpha} \frac{\partial z^{\alpha}}{\partial y^l} \frac{\partial^2 z^{\alpha}}{\partial y^s \partial y^n} + \sum_{\alpha} \frac{\partial z^{\alpha}}{\partial y^s} \frac{\partial^2 z^{\alpha}}{\partial y^l \partial y^n} \quad (6)$$

$$\frac{\partial g_{ln}}{\partial y^s} = \sum_{\alpha} \frac{\partial z^{\alpha}}{\partial y^l} \frac{\partial^2 z^{\alpha}}{\partial y^s \partial y^n} + \sum_{\alpha} \frac{\partial z^{\alpha}}{\partial y^n} \frac{\partial^2 z^{\alpha}}{\partial y^l \partial y^s} \quad (7)$$

$$\frac{\partial g_{sn}}{\partial y^l} = \sum_{\alpha} \frac{\partial z^{\alpha}}{\partial y^s} \frac{\partial^2 z^{\alpha}}{\partial y^l \partial y^n} + \sum_{\alpha} \frac{\partial z^{\alpha}}{\partial y^n} \frac{\partial^2 z^{\alpha}}{\partial y^l \partial y^s} \quad (8)$$

Now, Christoffel symbols of first and second kind are

$$[sn, l] = \frac{1}{2} \left(\frac{\partial g_{ls}}{\partial y^n} + \frac{\partial g_{ln}}{\partial y^s} - \frac{\partial g_{sn}}{\partial y^l} \right) = \sum_{\alpha} \frac{\partial z^{\alpha}}{\partial y^l} \frac{\partial^2 z^{\alpha}}{\partial y^s \partial y^n} \quad (9)$$

$$\Gamma_{sn}^t = \sum_{l=1}^n g^{tl} [sn, l] \quad (10)$$

Similarly, Christoffel symbols with other combination of indices can be calculated and substituted in Riemannian curvature tensor below to get the curvature defined by z coordinate system.

$$R_{srn}^t = \frac{\partial \Gamma_{sn}^t}{\partial y^r} - \frac{\partial \Gamma_{rn}^t}{\partial y^s} + \sum_{\mu=1}^n \Gamma_{sn}^{\mu} \Gamma_{pr}^t - \sum_{\mu=1}^n \Gamma_{rn}^{\mu} \Gamma_{ps}^t \quad (11)$$

Curvature of x coordinate system with respect to curved z coordinate system:

Metric equations which are needed to calculate Christoffel symbol Γ_{sn}^t are

$$g_{ls} = \sum_{\alpha} \frac{\partial x^{\alpha}}{\partial z^l} \frac{\partial x^{\alpha}}{\partial z^s}, \quad g_{ln} = \sum_{\alpha} \frac{\partial x^{\alpha}}{\partial z^l} \frac{\partial x^{\alpha}}{\partial z^n}, \quad g_{sn} = \sum_{\alpha} \frac{\partial x^{\alpha}}{\partial z^s} \frac{\partial x^{\alpha}}{\partial z^n}, \quad \text{and } g^{tl} = \sum_{\beta} \frac{\partial z^t}{\partial x^{\beta}} \frac{\partial z^l}{\partial x^{\beta}} \quad (12)$$

In the equations from equation (5) to equation (9), z and y can be replaced by x and z to get equation (13), which give us the curvature defined by x coordinate system with respect to the curvature of z coordinate system calculated using equation (11).

$$R_{srn}^t = \frac{\partial \Gamma_{sn}^t}{\partial y^r} - \frac{\partial \Gamma_{rn}^t}{\partial y^s} + \sum_{\mu=1}^n \Gamma_{sn}^{\mu} \Gamma_{pr}^t - \sum_{\mu=1}^n \Gamma_{rn}^{\mu} \Gamma_{ps}^t \quad (13)$$

The curvature defined by equation (13) gives us any possible curvature of universe beyond the observable flat universe. The meaning of this curvature in the context of evolution explained in section 5, is described in subsection 5.3.

5 Evolution of Gravitationally Bound Structures

A generic idea on the evolution of gravitationally bound structures and its consequences are discussed here. Let us say there are n classifications of gravitationally bound structures corresponding to order 1, order 2, ..., order n . Order 1 to order n are the epoch in which, still interacting associated gravitationally bound structures are formed. As seen in fig. 4 below, smaller gravitationally bound structures, as they cease to interact, give rise to larger gravitationally bound structures. This method of evolution applies from smallest possible to largest sustainable gravitationally bound structures, that is, from order 1 to order n .

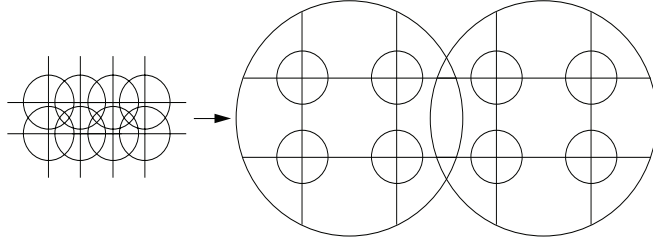


Figure 4: Evolution of gravitationally bound structures; left side image shows interacting objects of some order and right side image shows that these interacting objects have become independent.

For explanation below, two non-interacting smaller gravitationally bound structures in the intersecting region of two larger gravitationally bound structures can be considered (see fig. 5).

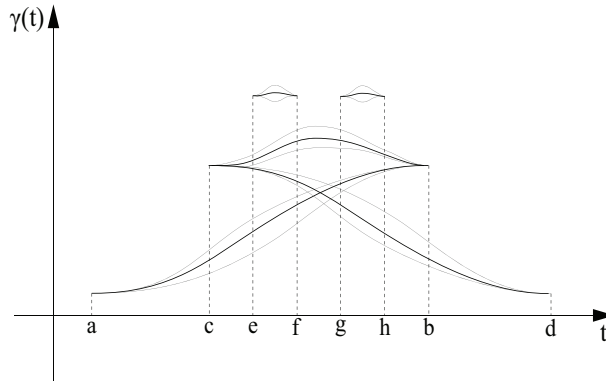


Figure 5: Geodesic arrangement – equation (2) is employed here to explain the evolution of objects.

So, the sum of differentiation of energy functional with respect to u for these paths is

$$\begin{aligned}
& \frac{dE(\bar{\alpha}(u))}{du} \Big|_a^b + \frac{dE(\bar{\alpha}(u))}{du} \Big|_e^f + \frac{dE(\bar{\alpha}(u))}{du} \Big|_c^b + \frac{dE(\bar{\alpha}(u))}{du} \Big|_g^h + \frac{dE(\bar{\alpha}(u))}{du} \Big|_c^d = \\
& - \int_a^b \sum_{t=1}^n \frac{\partial \alpha^t(0, t)}{\partial u} \left[\sum_{r=1}^n g_{tr}(\gamma(t)) \frac{d^2 \gamma^r}{dt^2} + \sum_{i,j=1}^n [ij, t](\gamma(t)) \frac{d\gamma^i}{dt} \frac{d\gamma^j}{dt} \right] dt \\
& - \int_e^f \sum_{t=1}^n \frac{\partial \alpha^t(0, t)}{\partial u} \left[\sum_{r=1}^n g_{tr}(\gamma(t)) \frac{d^2 \gamma^r}{dt^2} + \sum_{s,u=1}^n [su, t](\gamma(t)) \frac{d\gamma^s}{dt} \frac{d\gamma^u}{dt} \right] dt \\
& - \int_c^b \sum_{t=1}^n \frac{\partial \alpha^t(0, t)}{\partial u} \left[\sum_{r=1}^n g_{tr}(\gamma(t)) \frac{d^2 \gamma^r}{dt^2} + \sum_{k,l=1}^n [kl, t](\gamma(t)) \frac{d\gamma^k}{dt} \frac{d\gamma^l}{dt} \right] dt \\
& - \int_g^h \sum_{t=1}^n \frac{\partial \alpha^t(0, t)}{\partial u} \left[\sum_{r=1}^n g_{tr}(\gamma(t)) \frac{d^2 \gamma^r}{dt^2} + \sum_{v,w=1}^n [vw, t](\gamma(t)) \frac{d\gamma^v}{dt} \frac{d\gamma^w}{dt} \right] dt \\
& - \int_c^d \sum_{t=1}^n \frac{\partial \alpha^t(0, t)}{\partial u} \left[\sum_{r=1}^n g_{tr}(\gamma(t)) \frac{d^2 \gamma^r}{dt^2} + \sum_{m,n=1}^n [mn, t](\gamma(t)) \frac{d\gamma^m}{dt} \frac{d\gamma^n}{dt} \right] dt
\end{aligned} \tag{14}$$

For equation (14) to become 0, the condition below must hold.

$$\begin{aligned}
& \left[\sum_{r=1}^n g_{tr}(\gamma(t)) \frac{d^2 \gamma^r}{dt^2} + \sum_{i,j=1}^n [ij, t](\gamma(t)) \frac{d\gamma^i}{dt} \frac{d\gamma^j}{dt} \right] + \left[\sum_{r=1}^n g_{tr}(\gamma(t)) \frac{d^2 \gamma^r}{dt^2} + \sum_{s,u=1}^n [su, t](\gamma(t)) \frac{d\gamma^s}{dt} \frac{d\gamma^u}{dt} \right] \\
& + \left[\sum_{r=1}^n g_{tr}(\gamma(t)) \frac{d^2 \gamma^r}{dt^2} + \sum_{k,l=1}^n [kl, t](\gamma(t)) \frac{d\gamma^k}{dt} \frac{d\gamma^l}{dt} \right] + \left[\sum_{r=1}^n g_{tr}(\gamma(t)) \frac{d^2 \gamma^r}{dt^2} + \sum_{v,w=1}^n [vw, t](\gamma(t)) \frac{d\gamma^v}{dt} \frac{d\gamma^w}{dt} \right] \\
& + \left[\sum_{r=1}^n g_{tr}(\gamma(t)) \frac{d^2 \gamma^r}{dt^2} + \sum_{m,n=1}^n [mn, t](\gamma(t)) \frac{d\gamma^m}{dt} \frac{d\gamma^n}{dt} \right] = 0
\end{aligned}$$

Γ_{ij}^p , Γ_{su}^p , Γ_{kl}^p , Γ_{vw}^p , and Γ_{mn}^p are introduced here to write the above equation in standard form.

$$\begin{aligned}
& \left[\frac{d^2 \gamma^p}{dt^2} + \sum_{i,j=1}^n \Gamma_{ij}^p(\gamma(t)) \frac{d\gamma^i}{dt} \frac{d\gamma^j}{dt} \right] + \left[\frac{d^2 \gamma^p}{dt^2} + \sum_{s,u=1}^n \Gamma_{su}^p(\gamma(t)) \frac{d\gamma^s}{dt} \frac{d\gamma^u}{dt} \right] + \left[\frac{d^2 \gamma^p}{dt^2} + \sum_{k,l=1}^n \Gamma_{kl}^p(\gamma(t)) \frac{d\gamma^k}{dt} \frac{d\gamma^l}{dt} \right] \\
& + \left[\frac{d^2 \gamma^p}{dt^2} + \sum_{v,w=1}^n \Gamma_{vw}^p(\gamma(t)) \frac{d\gamma^v}{dt} \frac{d\gamma^w}{dt} \right] + \left[\frac{d^2 \gamma^p}{dt^2} + \sum_{m,n=1}^n \Gamma_{mn}^p(\gamma(t)) \frac{d\gamma^m}{dt} \frac{d\gamma^n}{dt} \right] = 0
\end{aligned} \tag{15}$$

Rearranging equation (15), we get

$$\begin{aligned}
& \left[\frac{d^2 \gamma^p}{dt^2} + \sum_{s,u=1}^n \Gamma_{su}^p(\gamma(t)) \frac{d\gamma^s}{dt} \frac{d\gamma^u}{dt} \right] + \left[\frac{d^2 \gamma^p}{dt^2} + \sum_{v,w=1}^n \Gamma_{vw}^p(\gamma(t)) \frac{d\gamma^v}{dt} \frac{d\gamma^w}{dt} \right] = - \left[\frac{d^2 \gamma^p}{dt^2} + \sum_{k,l=1}^n \Gamma_{kl}^p(\gamma(t)) \frac{d\gamma^k}{dt} \frac{d\gamma^l}{dt} \right] \\
& - \left[\frac{d^2 \gamma^p}{dt^2} + \sum_{i,j=1}^n \Gamma_{ij}^p(\gamma(t)) \frac{d\gamma^i}{dt} \frac{d\gamma^j}{dt} \right] - \left[\frac{d^2 \gamma^p}{dt^2} + \sum_{m,n=1}^n \Gamma_{mn}^p(\gamma(t)) \frac{d\gamma^m}{dt} \frac{d\gamma^n}{dt} \right]
\end{aligned} \tag{16}$$

³In equation (14), n in subscript of \sum refers to n^{th} component of γ and n in superscript refers to summation limit. This holds for equations up to equation (16).

For the intersecting region of two larger gravitationally bound structures, we can use equation (4). Substituting equation (4) in equation (16), we get

$$\left[\frac{d^2\gamma^p}{dt^2} + \sum_{s,u=1}^n \Gamma_{su}^p(\gamma(t)) \frac{d\gamma^s}{dt} \frac{d\gamma^u}{dt} \right] + \left[\frac{d^2\gamma^p}{dt^2} + \sum_{v,w=1}^n \Gamma_{vw}^p(\gamma(t)) \frac{d\gamma^v}{dt} \frac{d\gamma^w}{dt} \right] = 0 \quad (17)$$

$$\left[\frac{d^2\gamma^p}{dt^2} + \sum_{s,u=1}^n \Gamma_{su}^p(\gamma(t)) \frac{d\gamma^s}{dt} \frac{d\gamma^u}{dt} \right] = - \left[\frac{d^2\gamma^p}{dt^2} + \sum_{v,w=1}^n \Gamma_{vw}^p(\gamma(t)) \frac{d\gamma^v}{dt} \frac{d\gamma^w}{dt} \right] \quad (18)$$

Equation (18) is the condition when smaller gravitationally bound structures cease to interact. The fact that we have used equation (4) for the intersecting region of two larger gravitationally bound structures to derive equation (18) is incidentally the proof that larger gravitationally bound structures which did not exist when the smaller gravitationally bound structures were intersecting, has formed.

For any n , expansion of independent objects of order $n - 1$ ⁴ inside interacting objects of order n can be described by Standard Model of Cosmology (Susskind, 2013c). While the expansion of independent objects inside interacting objects obey Standard Model, expansion of universe obey the evolution of gravitationally bound structures described in this section.

In Newtonian two-body problem, say for a binary system, equation of motion can be easily obtained. This equation of motion which expresses acceleration in terms of position and velocity suit the needs of exact theory. On the contrary, for General Relativity, approximation methods are preferred as deriving equations of motion in the way exact theory demands is difficult. For General Relativity, apart from Post-Newtonian approximations, Numerical Relativity simulations, Gravitational Self-Force computations, recently developed Effective One Body formalism, and various combinations of these are discussed in Damour (2014a,b). For both Newtonian and General Relativity two-body problems, observations i.e., binary systems, including binary systems of neutron stars and black holes were already in place. This in fact was the driving factor to come up with the required equations of motion to validate the theories with observed facts.

Unlike the aforementioned two-body problem in General Relativity, two-body problem discussed in this section is motivated by the prospect of a consequence, in this case, specifically, as to how the gravitationally bound structures evolve. So, two body approximations which primarily validates General Theory of Relativity using observations and/or experiments is by purpose different from the two-body problem discussed in this section. And also considering the limitations in observational data for this evolution pattern at this point of time, formulations for this two-body problem, in a way which adheres to exact theory is out of scope of this paper. To get a more detailed understanding of approximate solutions to general relativity, refer Poisson & Will (2014).

With the details inferred in this section, accelerating expansion of universe, cosmic inflation, large-scale structure of universe, collapse⁵ of gravitationally bound structures, and distribution of matter and antimatter are discussed in the subsections below.

5.1 Accelerating Expansion of Universe and Dark Energy

I. In the explanation below, objects of order n refer to interacting objects formed in order n , and objects of order $n - 1$ refer to independent objects inside interacting objects of order n . Both these objects are relatively used to explain accelerating expansion of universe in this subsection and cosmic inflation in subsection 5.2. Though, objects of order n in this evolution pattern refer to the largest sustainable objects in our universe, it is used here for explanation as interacting objects of any order.

- A. From order 2 to order n , interacting groups become larger in geometry and the mass densities of larger groups are always lower than that of its immediate predecessor. This proportionately decreases the gravitational attraction between larger gravitationally bound

⁴Objects of an order refer to the objects formed in that order (epoch).

⁵Collapse of an object here refers to the object losing its structure, but still exists.

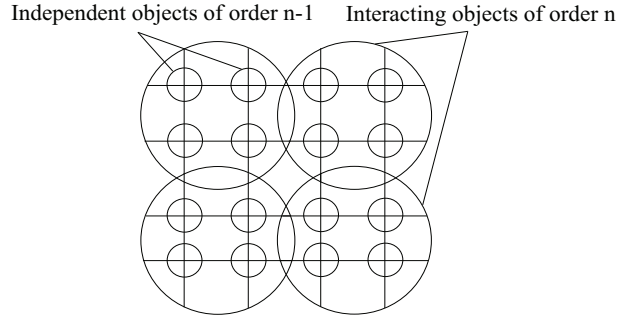


Figure 6: Accelerating expansion of universe

structures compared to its immediate predecessors, causing the expanding universe to accelerate.

- B. If independent objects of order $n - 1$ are still expanding inside the newly formed objects of order n , then the former delays latter from becoming independent. Actually, expanding independent objects do not slow down the receding rates of interacting objects, but they just delay interacting objects from becoming independent.
- C. Then, in increasing steps, receding rate of independent objects of order $n - 1$ increases due to decrease in their mass densities. A short proof using details in Susskind (2013a) is provided below.

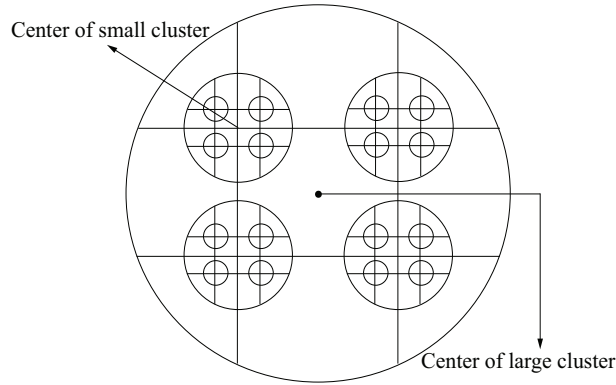


Figure 7: Accelerating expansion of independent objects

$$D_{ab} = a(t)\Delta X_{ab}$$

$$V_{ab} = \frac{da(t)}{dt}\Delta X_{ab}$$

$$\text{Hubble function} = \frac{V_{ab}}{D_{ab}} = \frac{\frac{da(t)}{dt}}{a(t)} \quad (19)$$

In equation (19), ΔX_{ab} cancels each other. As discussed in Susskind (2013a), Hubble function is independent of actual distances between galaxies in galaxy lattice. So, for any $n > 1$, galaxy lattice in this lecture can be used to describe objects of order $n - 1$.

As shown in fig. 7, when looked at from the center of small or big cluster, mass inside the respective cluster is isotropic. So, total mass of all objects of order $n - 1$ inside any interacting cluster is assumed to be concentrated at center of the cluster. Though in fact it is

the opposite, the center of cluster is considered to be not moving for mathematical ease. The equation for acceleration to distance ratio is

$$\frac{\frac{d^2 a(t)}{dt^2}}{a(t)} = -\frac{4}{3}\pi\rho G \quad (20)$$

The negative second derivative says, expanding independent objects of order $n - 1$ will eventually slow down. If the mass density is low, RHS = (small negative value), and so the expansion slows down slowly. Therefore, in increasing steps, expansion of independent objects of order $n - 1$ accelerates.

- D. The combined action of independent and interacting objects should be considered as a single phenomenon, decreasing the mass density of universe. For each step, the time delay, objects of order $n - 1$ induces to objects of order n from becoming independent is same. Yet, the decrease in mass density causes expanding universe to accelerate.

II. Another consequence that follows is that the need for dark energy to primarily account for the accelerating expansion of universe is not required in this evolution.

5.2 Cosmic Inflation

In the very early universe before order 1, gravitationally bound structures are not formed. Consequently, they cannot be grouped together. So, when gravitationally bound structures corresponding to order 1 are formed, they are already non-interacting objects. So, by equation (18), gravitationally bound structures corresponding to order 1 and order 2 are formed simultaneously. From order 2 to order n they are formed in the increasing order of time. This explains in the infant universe just after big bang, an exponential expansion, which slowed after that. Simultaneous formation of gravitationally bound structures corresponding to order 1 and order 2 substantially reduced the mass density of universe just after big bang, before getting into accelerating expansion at a much slower rate.

Furthermore, as objects associated with order 1 and order 2 start expanding at same time, expansion of former considerably delays the latter from becoming independent. But eventually objects associated with order 2 become independent because of relatively higher expansion rate than that of order 1 objects. So, inflation starts precisely at time t_i , when objects of order 1 and order 2 are formed, and ends precisely at time t_f , when objects of order 2 become independent.

Inflationary theory as described in Susskind (2013b), invokes a hypothetical scalar field to describe the potential energy curve shown in fig. 8.

$$\frac{d^2 \phi(t)}{dt^2} + 3H \frac{d\phi(t)}{dt} = F(\phi) \quad (21)$$

Where, $F(\phi)$ is the tendency of the field to move towards lower potential energy.

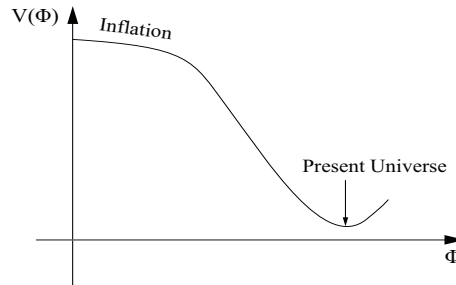


Figure 8: Potential energy curve

As shown in fig. 8, the hypothetical dark energy is employed to explain the accelerating expansion observed in our present universe. But, as inferred from the evolution of gravitationally bound structures, inflation and observed accelerating expansion are accounted by gravitational forces itself. Therefore, the hypothetical scalar field and dark energy becomes irrelevant in this context.

Though, the cause of inflation differs in this context, there are similarities they both share in explaining the phenomenon. As discussed in Susskind (2013b), inflation should have happened over a sufficient amount of time to simultaneously account for flatness of observable universe and dilution of magnetic monopoles. Quantitatively, this means that e^{Ht} in equation (22) should be at least e^{60} .

$$a = e^{Ht} \tag{22}$$

Objects of order 1 and order 2 simultaneously initiate their expansion and consequently, objects of order 1 considerably delays objects of order 2 from becoming independent. This is in concurrence with the prolonged inflation illustrated by the potential energy curve in fig. 8.

As we know, inflationary theory accounts for two cosmological principles, isotropy and homogeneity of observable universe, and in addition also accounts for the observed flatness of space and dilution of magnetic monopoles.

- **Isotropy:** Equation (19) which explains the contraction or expansion of galaxy lattice is the basis for standard cosmology theory. Now, that clusters and super clusters are observational facts, the process of forming and certainly arrangement of clusters decide the correctness of isotropy. As shown in fig. 6, the direction we look at from earth does matter, rendering the conception of isotropy obsolete in this context.
- **Homogeneity:** The evolution described in this paper, with the expansion of objects constrained to their own clusters, causes a disparity in their expansion rates. Therefore, the homogeneity of the entirety of space is as obsolete as isotropy in this context.
- **Flatness of Space:** In this context, irrespective of observable universe being flat or curved, there are curvatures on scales larger than observable universe, due to gravitationally bound structures of relatively recent orders. Subsection 5.3 contains a brief discussion about the large-scale structure of universe, inferred from this evolution pattern. This inflation does not explain the flatness in our observable universe. A statement about the cause of this observed flatness is added as the last paragraph in conclusion. So, the condition below for inflation, as discussed in Lesgourgues (2006, pp. 6 to 8) is not required here.

$$\frac{a_f}{a_i} \geq \frac{a_o}{a_f}$$

Therefore, the exactly exponential De Sitter expansion during inflation for simplifying calculations to primarily solve flatness problem is not discussed here. Furthermore, as discussed in Lesgourgues (2006, pp. 6 to 8), number of inflationary e-folds should be greater than or equal to the number of post-inflationary e-folds.

$$N_f - N_i \geq N_o - N_f$$

For solving observable flatness problem, inflation could be arbitrarily long. On the contrary, inflation here has fixed constraints, defined by t_i and t_f .

- **Dilution of Magnetic Monopoles:** This inflation, like the inflationary theory (Susskind, 2013b) can explain the dilution of magnetic monopoles

Put together, the evolution pattern discussed in section 5 does not accommodate isotropy, homogeneity, and flatness of universe which inflation theories historically accounted for. Yet, this pattern naturally explains inflation in the early universe which can still explain the dilution of magnetic monopoles.

In this evolution pattern, though the same mechanism which drives both cosmic inflation and accelerating expansion of universe looks similar to quintessence proposal, it is just the gravity with different cosmological principles here that explains both cosmic inflation and accelerating expansion of universe.

5.3 Large-scale Structure of Universe

For observational purposes, discussion on the geometry of universe inferred from this evolution is limited to our own epoch. Let us assume here, order n corresponds to the largest interacting objects now. The geometry of space will be like the illustration in fig. 6. Each of the interacting objects will have geometry like the illustration in fig. 7.

The evolution process, which forms interacting objects by grouping independent objects, makes it evident that the objects of recent orders will be less in number. Consequently, number of interacting objects in our epoch will be the least compared to objects of all other orders.

Let us say that the observable flat universe is an object of order $n - l$, where $l = 1, \dots, n + 2$, that is, from order 2 to order $n - 1$. Then, section 4 helps us to calculate the curvature of x coordinate system (see fig. 3), that is, curvature of objects of order $(n - l) + 1$. Implications it has on observational astronomy to study the geometry of space is added in conclusion.

To get an idea about the curvature on the scale of order n , a pictorial representation of the curvature embedded in 3D Euclidean space, for four interacting objects of order n is sketched below.

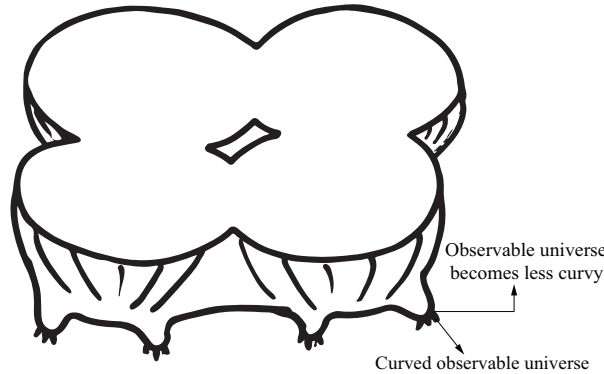


Figure 9: Large-scale structure of universe

5.4 Collapse of Gravitationally Bound Structures

As discussed in subsection 5.1 (see fig. 7), receding rate of larger cluster's objects is higher than the receding rate of smaller cluster's objects. Consequently, objects of order 1 at some point of time will first stop to recede from each other, and will start to collapse. This will be followed by the collapse of order 2, order 3, ..., order n objects in chronological order.

To understand this, let us say the larger cluster's objects are of order 2 classification and smaller cluster's objects are of order 1 classification. Then, when objects of order 1 are collapsed, the structure in fig. 7 is transformed as below

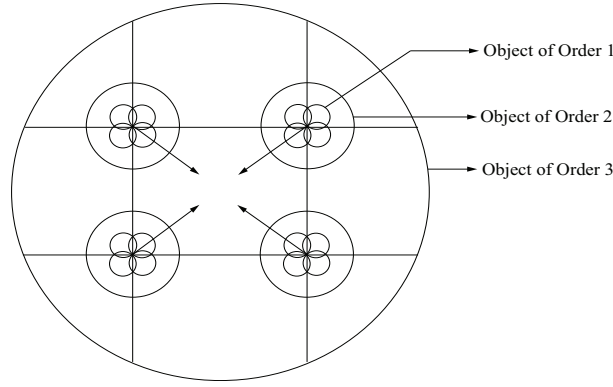


Figure 10: Shows the collapse of order 1 and order 2 objects. As long as objects of order 1 are collapsed to a single gravitationally bound structure, albeit they have collided, they continue to exist.

The universe expansion from big bang, and eventual collapse is symmetrical in nature. Though, collapse of order 1 objects will be followed by collapse of order 2 objects, by reversing the logic used for cosmic inflation, we can presume that objects of order 1 and order 2 will cease to exist at same time. So, fig. 10 is transformed as below

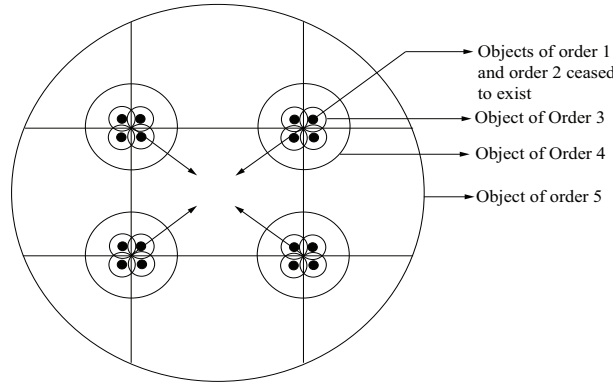


Figure 11: Using this evolution pattern for object birth⁶ and death⁷, when objects of order 3 collide, objects of order 1 and order 2 will have ceased to exist. Similar to this, when objects of order 4 collide, objects of order 3 will have ceased to exist and so on.

Eventually, objects of all orders will be dead due to collision of objects. This collision of objects will cause the temperature of universe to rise substantially.

5.5 Distribution of Matter and Antimatter

In the treatment of Riemannian metrics in Spivak (1999), geodesics are the critical points for the energy functional. If energy functional is negative, i.e. $E(\gamma(t)) = -\frac{1}{2} \int_a^b \left\langle \frac{d\gamma}{dt}, \frac{d\gamma}{dt} \right\rangle dt$, then equation (2) becomes

$$\frac{dE\bar{\alpha}(u)}{du} \Big|_a^b = - \int_a^b \sum_{t=1}^n \frac{\partial \alpha^t(0, t)}{\partial u} \times - \left[\sum_{r=1}^n g_{tr}(\gamma(t)) \frac{d^2 \gamma^r}{dt^2} + \sum_{i,j=1}^n [ij, t](\gamma(t)) \frac{d\gamma^i}{dt} \frac{d\gamma^j}{dt} \right] dt \quad (23)$$

⁵Birth of order 1 objects refers to the forming of independent objects in order 1. Birth of other objects refers to the forming of interacting objects in their respective orders.

⁶Death of objects is used to indicate that the objects eventually will cease to exist after collapse.

So here, $\gamma(t)$ should satisfy the equation,

$$-\left[\sum_{r=1}^n g_{tr}(\gamma(t)) \frac{d^2 \gamma^r}{dt^2} + \sum_{i,j=1}^n [ij,t](\gamma(t)) \frac{d\gamma^i}{dt} \frac{d\gamma^j}{dt} \right] = 0 \quad (24)$$

The negative energy functional here is similar to the negative-energy state of electrons, noted in the prediction of positrons (Dirac, 1933). Consequently, equation (24) is the critical point of this energy functional on Riemannian manifold formed by antimatter. So, the positive and negative energy functional correspond to the matter and antimatter region of curvature.

If n is some arbitrary number, multiplying equation (18) by n on both sides, we get

$$n \left[\frac{d^2 \gamma^p}{dt^2} + \sum_{s,u=1}^n \Gamma_{su}^p(\gamma(t)) \frac{d\gamma^s}{dt} \frac{d\gamma^u}{dt} \right] = -n \left[\frac{d^2 \gamma^p}{dt^2} + \sum_{v,w=1}^n \Gamma_{vw}^p(\gamma(t)) \frac{d\gamma^v}{dt} \frac{d\gamma^w}{dt} \right] \quad (25)$$

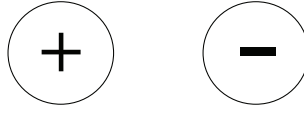


Figure 12: Distribution of matter and antimatter in independent objects: This means that when objects become independent or in case of order 1, when they are just formed, there are equal number of matter objects as that of antimatter objects.

Let x be the total number of intersecting regions, and n here be the total number of intersecting objects. Generalizing equation (4) for all intersecting objects, we get

$$\sum_{i=1}^x \text{Geodesic equation of } i^{\text{th}} \text{ intersecting region} = - \sum_{i=1}^n \text{Geodesic equation of } i^{\text{th}} \text{ intersecting object} \quad (26)$$

Multiplying equation (26) by -1 on both sides, we get

$$- \sum_{i=1}^x \text{Geodesic equation of } i^{\text{th}} \text{ intersecting region} = \sum_{i=1}^n \text{Geodesic equation of } i^{\text{th}} \text{ intersecting object} \quad (27)$$

Distribution of matter and antimatter in intersecting objects does not obey either equation (26) or equation (27). It obeys both equation (26) and equation (27). Consequently, for a single intersecting pair, there is an equal sharing of matter and antimatter objects. Graphically, it can be represented as shown in fig. 13.

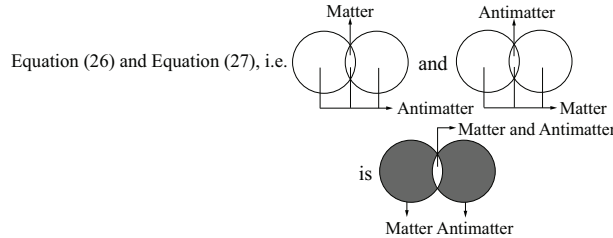


Figure 13: Distribution of matter and antimatter in intersecting objects: In case of intersecting region which obeys both equation (26) and equation (27), matter and antimatter are shared in that region. Whereas, there are two shaded regions and so, matter and antimatter are shared by separation in these two regions.

From the discussion in section 5, we can infer that when objects become independent or in case of order 1, when they are just formed, they lie within the intersecting region of newly formed objects. The dynamics of matter and antimatter objects during the simultaneous formation of order 1 and order 2 objects and during the formation of order 3 objects are shown in fig. 14 and fig. 15.

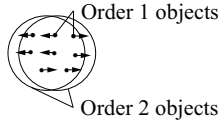


Figure 14: Simultaneous formation of order 1 and order 2 objects

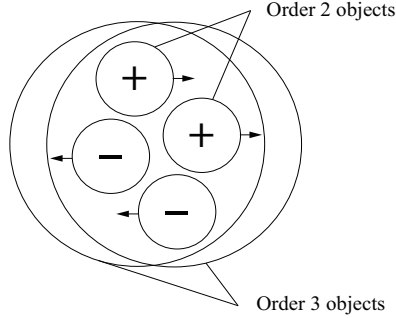


Figure 15: Formation of order 3 objects: To obey equation (25), we can see from fig. 14 and fig. 15, in each step, equal number of independent matter and antimatter objects move away from each other to form equal number of next order independent matter and antimatter objects.

For $x > 1$, if two objects of order $n - x$ are observed to be collided, we can safely presume at least two order $n - 1$ objects are collided. The collided objects of order $n - x$ have to obey both equation (26) and equation (27). So, matter and antimatter in the collided region of these objects has to come from a matter and antimatter object of order $n - 1$ and it further says that we are in an epoch, where order n objects are becoming independent.

5.5.1 Inferences

Let N_{e-} and N_{e+} be the number of electrons and positrons. As discussed in Susskind (2013d), in the very early universe at high temperatures, electrons and positrons annihilate to become photons. Then the photons loose energy by scattering and heating the universe. So, they won't be able to collide with high energies to produce back electrons and positrons.

So, if $N_{e-} = N_{e+}$ in the very early universe, what is the reason for $N_{e-} \gg N_{e+}$ in today's observable universe? There was never an anti-nuclei detected in cosmic rays even from far away galaxies. This is suggestive of electrons dominance over positrons on a large scale.

From the pattern discussed in subsection 5.5 (see fig. 13), observable universe should lie within the shaded matter region of order n objects to account for the observed dominance of electrons over positrons.

It is an experimental fact that charge of electron is equal and opposite to the charge of proton. In today's observable universe, number of protons and electrons are equal. So, universe appears to be electrically neutral. Similarly, charge of positron is equal and opposite to the charge of antiproton. It is natural to expect, and considering the electrically neutral behavior of our observable universe, it is highly likely that there will be equal number of positrons and antiprotons in the antimatter region of universe.

Electrons and protons are bonded together by hydrogen atom which is electrically neutral. Similarly, positrons and antiprotons could be bonded together by antihydrogen atom. The fact that antihydrogen atom was never detected in cosmic rays substantiates that we are reasonably far away from antimatter objects.

Few questions related to matter-antimatter distribution are discussed below.

Why we haven't observed an antihydrogen atom in our observable universe?

In the model discussed here, matter dominates our observable universe. So, few antimatter particles present here are annihilated by these matter particles and become photons. Hydrogen being the most abundant element in the universe, cancels out the few antihydrogen atoms in our observable universe.

Why matter escaped total annihilation in the universe?

In this model, not just matter, both matter and antimatter escaped total annihilation in the universe. In general, independent matter and antimatter objects move away from each other to form higher order independent matter and antimatter objects (see fig. 15). In the early smaller universe, for independent order 1 objects, there is a higher possibility of matter and antimatter objects getting collided during the crossover between intersecting order 2 objects, resulting in higher annihilations. As the universe expands, possibility of matter-antimatter collision reduces for higher order objects, resulting in lesser annihilations and correspondingly affects the production of photons.

What are the observational constraints on this hypothesis?

Total number of object classifications existing in our current epoch should be understood to get an idea about the region where antimatter objects are located in the universe. While we may or may not be able to look at antimatter objects directly depending on the scale of universe, there could be many interesting indirect observational methods to prove their existence.

6 Related Numerical Relativity Results

Results from three recently published papers on numerical relativity are compared with the evolution of universe discussed here and inferences are made.

6.1 Results in Giblin et al. (2016)

As mentioned in Giblin et al. (2016), one of the main predictions of FLRW universe is that any path on a constant t surface, no matter the shape, has a proper length that scales with the scale factor of universe.

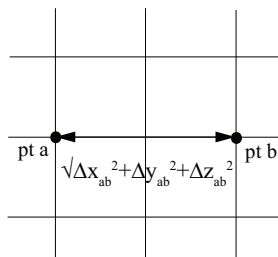


Figure 16: Standard model of cosmology – lattice

In standard model of cosmology, expansion of universe is plotted with t along x -axis and a along y -axis. So, scale factor a gives the expansion rate of universe. This says that, as mentioned in equation (19), the distance between pt a and pt b, $\sqrt{\Delta x_{ab}^2 + \Delta y_{ab}^2 + \Delta z_{ab}^2}$ does not matter (as it cancels out).

A numerical relativity result calculated by Giblin et al. (2016) is in contrast to the aforementioned idea. They have defined a set of arbitrary paths on their constant t hypersurfaces. They have calculated the proper length of those paths to track the ratio of those lengths as a function of time to see deviations from FLRW behavior, and found that

$$\frac{\sqrt{\Delta x_{ab}^2 + \Delta y_{ab}^2 + \Delta z_{ab}^2} \text{ at time } t_1}{\sqrt{\Delta x_{ab}^2 + \Delta y_{ab}^2 + \Delta z_{ab}^2} \text{ at time } t_2} \neq \frac{\sqrt{\Delta x_{ab}^2 + \Delta y_{ab}^2 + \Delta z_{ab}^2} \text{ at time } t_2}{\sqrt{\Delta x_{ab}^2 + \Delta y_{ab}^2 + \Delta z_{ab}^2} \text{ at time } t_3}$$

Where,

$$\frac{t_1}{t_2} = \frac{t_2}{t_3}$$

That is, expansion rate of universe depends on the distance between a and b, contradicting the main prediction of FLRW universe.

Two important details can be observed from fig. 3 in Giblin et al. (2016).

1. It shows that the growth of the proper length of these paths depend on the length of path, and not just some scale factor, a .
2. Further it suggests that this departure is more important at smaller distances than at larger distances.

First result can be compared to the evolution pattern discussed in this paper. To highlight the difference in distance between objects of different orders, fig. 7 is edited as below

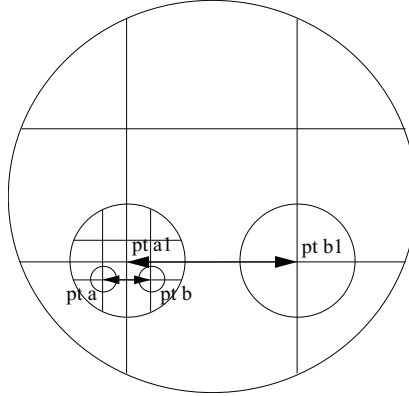


Figure 17: Distance between objects

In fig. 7, the claim that the expansion rate of larger cluster is higher than that of small cluster is substantiated by the first result from fig. 3 in Giblin et al. (2016). It also says, if inhomogeneities are present in the universe, objects recede from each other depending on the distance between them. Here, it means difference in ΔX_{ab} and ΔX_{a1b1} affects the expansion rate of small and large cluster proportionately.

The initial conditions in Giblin et al. (2016) describes an universe expanding at a constant rate across a set of points, each representing slightly different volumes. This falls in line with the evolution discussed in this paper, as objects of order 1 and order 2 start receding from their respective objects at same time, t_i (order 1 and order 2 are formed simultaneously at time, t_i). So, objects of order 1 and order 2 or in general any independent and intersecting objects pair start receding from their respective objects at same rate.

Essence of the discussion in this subsection is that the distance $\sqrt{\Delta x_{ab}^2 + \Delta y_{ab}^2 + \Delta z_{ab}^2}$ does matter, which means that whether the Newton's standard model of cosmology lattice is a galaxy lattice or a galaxy cluster lattice, or a lattice of other cluster classification does matter in our universe. So, it means geodesics, a measure of distance in Riemannian manifold is significant in inferring the evolution of universe, as discussed here in this paper.

6.2 Results in Bentivegna & Bruni (2016)

When universe is evolved with FLRW background and with overdensity at some region using numerical relativity, the density contrast between the overdense region and FLRW background increases nonlinearly a little while after evolution and becomes unconstrainedly nonlinear after some time.

This can be noted from fig. 4 in Bentivegna & Bruni (2016). Compared to linear perturbation theory, for small values of the initial δi , the density contrast grows linearly with a , all the way through $a/a_i = 100$. For $\delta i = 10^{-2}$, there is a clear departure from this behavior, with the overdensity becoming nonlinear already at $a/a_i = 5$, and growing unbounded at $a/a_i \approx 96$.

We can apply this to the evolution discussed here (see fig. 7). As mentioned in subsection 5.1, the small and large cluster start expanding at same rate and the density contrast between them increases as the universe evolves.

1. If the initial density contrast between small and large cluster is small, then according to fig. 4 in Bentivegna & Bruni (2016), the increase in density contrast is negligible.
2. If the initial density contrast between small and large cluster is large, then the increase in density contrast is non-linear.

We can apply the second case above, and consider the overdense region as of order 1 objects and FLRW background as of order 2 objects, the density contrast between them increases nonlinearly. So, this happens for order 1 and order 2 pair, order 2 and order 3 pair, and so on. This supports the claim that the evolution pattern in this paper itself explains acceleration of expanding universe.

6.3 Results in Green & Wald (2014)

As mentioned in Green & Wald (2014), in the Λ CDM model, the space time metric g_{ab} of our universe is approximated by a FLRW metric $g_{ab}^{(0)}$. However, derivatives of g_{ab} are not close to the derivatives of $g_{ab}^{(0)}$. Geodesic equation has a Christoffel symbol which is made of first derivatives of g_{ab} and $g_{ab}^{(0)}$, and Riemannian curvature tensor is made of second derivatives of g_{ab} and $g_{ab}^{(0)}$. So, there can be significant difference in the behavior of geodesics and huge difference in curvature for these two metrics. Consequently, observable quantities in the actual universe may differ significantly from the corresponding observables in the FLRW model.

Green & Wald (2014) used the above argument to prove that anomalies in observables are mismatch between actual metric of universe and FLRW metric and not backreaction effect.

Inference is, this anomaly due to the significant differences in geodesics between g_{ab} and $g_{ab}^{(0)}$, whether we call it backreaction effect or not, explains the acceleration of expanding universe. In the context of this paper, $g_{ab}^{(0)}$ should be such that its Riemannian curvature tensor is close to this universe (see fig. 9), so that the $g_{ab}^{(0)}$ calculated values match exactly with the observed data. As mentioned in subsection 5.2, this universe is not isotropic and so the position of earth in our universe, from where we observe should also be considered.

6.4 Inferences

Conceptually, galaxy lattice in Newton's standard model of cosmology should be compared to the lattice below in this evolution pattern to understand its meaning here.

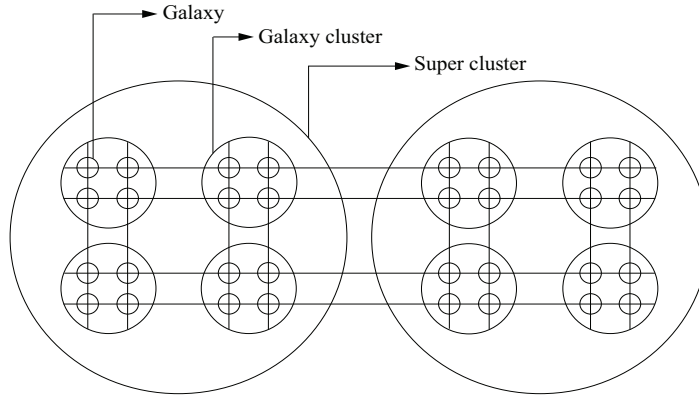


Figure 18: Newton's standard model of cosmology galaxy lattice is superimposed on the evolution pattern discussed in this paper. Clearly, distance between the galaxies is not constant. On the contrary, the distance between the galaxies increases from within galaxy clusters to between cluster of galaxies, and from between galaxy clusters to between super clusters and so on.

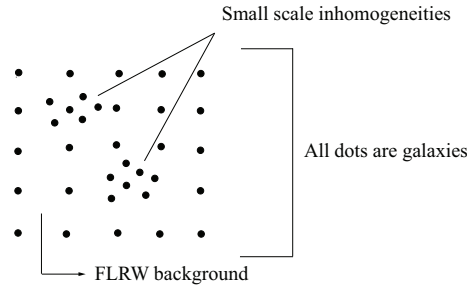


Figure 19: FLRW background with small scale inhomogeneities

In these numerical relativity calculations, they have essentially grouped together galaxies on small scale to find how galaxies are distributed on large scales of universe. But instead, galaxies should be grouped to find how galaxy clusters are arranged on large scales, and galaxy clusters should be grouped to find how super clusters are arranged on large scales, and so on.

Inhomogeneity in our universe is an observable fact (de Vaucouleurs, 1970; Broadhurst et al., 1990; Sylos Labini et al., 2009) and this has led contemporary cosmologists to contemplate the presence of inhomogeneity even in the early universe. As we acknowledge this, it is natural to expect that inhomogeneity exist between different scales, or orders in this context — between galaxies and galaxy clusters, and between galaxy clusters and super clusters, etc. So, as inhomogeneity exist between different orders of objects, it should also exist between order $n - 1$ and order n objects. As, there is inhomogeneity in the largest scale of universe, other two important cosmological principles like isotropy and flatness of universe does not hold true.

Observable universe, on large scales is flat, matching the homogeneously arranged galaxies in standard cosmology model galaxy lattice. As shown in fig. 18, studying the arrangement of galaxies based on object classification could help to understand the inhomogeneous nature in the arrangement.

7 Discussion

In the geometrical study of universe, most common investigations cover the flat, spherical, and hyperboloid spaces, as described in Susskind (2013e). Section 4 describes a method to study the geometry of space beyond observable flat universe by using the details available within the observable limit. In big scales, matter is electrically neutral. So, gravitational force alone is

considered to be the deciding force for the working of universe.

In Newton's standard model of cosmology, $\frac{da(t)}{a(t)}$ describes the expansion or contraction of galaxy lattice as defined by equation (19). Specifically, the ratio $\frac{da(t)}{a(t)}$, to explain the expansion or contraction of galaxy lattice is replaced in this paper by the evolution of gravitationally bound structures. As described in Susskind (2013c), equation of motion of our real universe, that is, mixed matter and radiation dominated universe is

$$\left(\frac{da(t)}{a(t)}\right)^2 = \frac{c_m}{a^3} + \frac{c_r}{a^4} \quad (28)$$

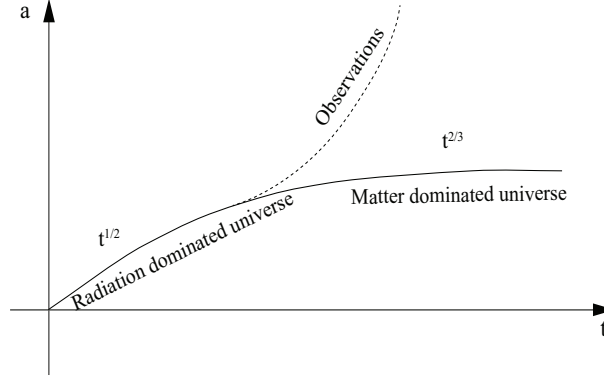


Figure 20: Comparison with standard model

To primarily account for the dotted line, that is, accelerating expansion of universe, dark energy was introduced. But, it has to do with the conception of galaxy lattice, which is replaced with the evolution of gravitationally bound structures in this paper, explain the accelerating expansion of universe.

This paper, though gives a variational approach to describe accelerating expansion of universe using evolution of gravitationally bound structures, does not elaborate the specifics of how corrections to Newtonian cosmology can be achieved. So, the purpose of this paper is not to correct, but to make contact with standard cosmological equations to an essential extent. The abstract nature of this paper is to make the understanding more generic against the naturally intuitive standard model.

8 Conclusion

In this paper, wherever collision or intersection of gravitationally bound structures is mentioned, it is implied that they are of same classification. Equation (4) derived in section 3 is the basis for analysis in all other sections. The primary nature of equation (4) in all other sections is a display of its generality which can be used to study varied geometrical dynamics.

In the analytical method discussed in section 4 to calculate the curvature of universe beyond our observable flat universe, for practical purposes, we can consider the gravitationally bound structures colliding in the observable flat region to be galaxy collisions. This method can be plausibly used to calculate the large-scale structure of universe, using interactions of gravitationally bound structures observed in our own epoch.

If observable universe is confirmed to be flat, then section 4 can be used to find the curvature of an object of order $(n - l) + 1$, which accommodates and whose expansion flattened our observable universe. On the contrary, as shown in fig. 9, if observable universe is curved, then we have to look at geometry, where the space starts becoming less curvy.

9 Acknowledgment

I am grateful to the anonymous reviewer in Foundations of Physics journal, for his efforts to provide elaborate and useful comments on this work.

References

- Bentivegna, E., & Bruni, M. 2016, Phys. Rev. Lett., 116, 251302, doi: 10.1103/PhysRevLett.116.251302
- Broadhurst, T. J., Ellis, R. S., Koo, D. C., & Szalay, A. S. 1990, Nature, 343, 726–728, doi: 10.1038/343726a0
- Damour, T. 2014a, in Fundamental Theories of Physics, Vol. 177, General Relativity, Cosmology and Astrophysics, 1st edn., ed. T. Bičák, J. & Ledvinka (Cham, Switzerland: Springer International Publishing), 111–145. https://link.springer.com/chapter/10.1007%2F978-3-319-06349-2_5
- . 2014b, in De Gruyter Studies in Mathematical Physics, Vol. 1, Frontiers in Relativistic Celestial Mechanics, 1st edn., ed. S. M. Kopeikin (Germany: De Gruyter), 1–38. <https://www.degruyter.com/view/books/9783110337495/9783110337495.1/9783110337495.1.xml>
- de Vaucouleurs, G. 1970, Science, 167, 1203–1213, doi: 10.1126/science.167.3922.1203
- Dirac, P. A. 1933, Nobel Lecture: Theory of Electrons and Positrons, Nobelprize.org. https://www.nobelprize.org/nobel_prizes/physics/laureates/1933/dirac-lecture.html
- Giblin, J. T., Mertens, J. B., & Starkman, G. D. 2016, Phys. Rev. Lett., 116, 251301, doi: 10.1103/PhysRevLett.116.251301
- Green, S. R., & Wald, R. M. 2014, Class. Quant. Grav., 31, 234003, doi: 10.1088/0264-9381/31/23/234003
- Lesgourgues, J. 2006, 3i^eme cycle de physique de Suisse romande, EPFL. https://lesgourg.github.io/courses/Inflation_EPFL.pdf
- Poisson, E., & Will, C. M. 2014, 10, Vol. 68, Gravity: Newtonian, Post-Newtonian, Relativistic, 1st edn. (Cambridge: Cambridge University Press), doi: 10.1063/PT.3.2951. <http://physicstoday.scitation.org/doi/10.1063/PT.3.2951>
- Spivak, M. 1999, A Comprehensive Introduction to Differential Geometry, 3rd edn., Vol. 1 (Houston, Texas: Publish or Perish, Inc.). <https://www.amazon.com/Comprehensive-Introduction-Differential-Geometry-Vol/dp/0914098705>
- Susskind, L. 2013a, The expanding (Newtonian) universe, Web page. <https://www.youtube.com/watch?v=P-medYaqVak&feature=youtu.be>
- . 2013b, Inflation, Web page. <https://www.youtube.com/watch?v=hAD0Y0TzLic&feature=youtu.be>
- . 2013c, Matter and radiation dominated universes, Web page. https://www.youtube.com/watch?v=938_TNP4aUs&feature=youtu.be
- . 2013d, Temperature history of the universe, Web page. <https://www.youtube.com/watch?v=GvhxamzVpN8&feature=youtu.be>
- . 2013e, Geometries of space: flat, spherical, hyperbolic, Web page. <https://www.youtube.com/watch?v=nJlWYDcGr8U&feature=youtu.be>
- Sylos Labini, F., Vasilyev, N. L., Pietronero, L., & Baryshev, Y. V. 2009, EPL (Europhysics Letters), 86, 49001, doi: 10.1209/0295-5075/86/49001
- Wisdom, J. 2003, Science, 299, 1865–1869, doi: 10.1126/science.1081406